INAF-Osservatorio astrofisico di Torino
Technical Report nr. 159

METIS 3-channel Configuration (draft)

Silvano Fineschi

Pino Torinese, 15 luglio 2012

METIS 3-channel Configuration

DRAFT

Silvano Fineschi
INAF – Astrophysical Observatory of Turin, Torino, Italy

issue 0
revision 0– draft 1
date of issue 15 July 2012

Page intentionally left blank

Distribution

Name	Organisation

Change Log

date	issue	revision	Paragraphs	reason for change
15/07/12	0	0	All	First release

Table of Contents

LIST OF FIGURES

LIST OF TABLES

1 Abstract

This document describes the 3-channel configuration of the METIS experiment. This configuration has been derived from the original 4-channel configuration as a consequence of the descoping of the He-imaging channel decided by ASI during the coordination meeting with Thales-Alenia Space on July the 13th, 2012.
In the 3-channel configuration, the following instrument components are descoped:

1. Al filter;
2. filter wheel mechanism.

In this configuration, the spectrographic channel is maintained with the following modification, with respect to the 4-channel configuration:

1. SVLS grating 1800 l/mm ⇒ 3600 l/mm:
2. eccentric ∅ 15 mm clear aperture on the ∅ 70 mm interference filter.

In the 3-channel configuration, the UV and EUV throughputs increase by the following factors, with respect to the 4-channel:

1. factor of 2.5 increase for the UV-imaging,
2. factor of 9.4 increase for the EV spectrography.

2 Revised 3-channel Experiment Science Objectives

The baseline 4-channel Multi-Element Telescope for Imaging and Spectroscopy - METIS – for the Solar Orbiter mission was designed to combine the imaging and spectroscopic capabilities of coronagraphs and spectrometers. With respect to the original METIS 4-channel configuration, the 3-channel configuration loses the HeII Ly-α imaging and the HI Ly-α spectrography, while it maintains the visible-light pB imaging, the HI Ly-α imaging and the HeII Ly-α spectrography. In addition, unlike in the 4-channel METIS, the 3-channel configuration may include also the MgX, 60.9 nm, spectrography.

Table 1 summarizes the different science performances of the 4- and 3-channel configurations.

4-channel	3-channel
linearly polarized K-corona imaging (590-650 nm)	linearly polarized K-corona imaging (590-650 nm)
narrow-band UV imaging HI Lyman α (121.6 nm)	narrow-band UV imaging HI Lyman α (121.6 nm)
narrow-band extreme UV imaging HeII (30.4 nm)	descoped
spectrography HI 121.6 nm (1st) HeII 30.4 nm (4th)	spectrography HeII 30.4 nm (2nd) MgX 60.9 nm (1st)

Table 1 Science performances of the 4- and 3-channel METIS configurations

3 Instrument Parameters

Table 2 summarizes the main differences (in red) between the 4- and 3-channel instrument components.

<table>
<tr><th colspan="2">Instrument Component</th><th>4-channel METIS configuration</th><th>3-channel METIS configuration</th></tr>
<tr><td colspan="2">M1 coating</td><td>UV-capped multilayer @ 30 nm</td><td>UV-capped multilayer @ 30 nm</td></tr>
<tr><td colspan="2">M2 coating</td><td>UV-capped multilayer @ 30 nm</td><td>Interference coating Al/MgF$_2$ @ 122 nm</td></tr>
<tr><td rowspan="3">SVLS grating</td><td>coating</td><td>UV-capped multilayer @ 30 nm</td><td>multilayer @ 30 nm (no UV-cap required)</td></tr>
<tr><td>ruling frequency</td><td>1800 lines/mm</td><td>3600 lines/mm</td></tr>
<tr><td>wavelengths</td><td>30.4 nm @ 4^{th}
121.6 nm @ 1^{st} order;</td><td>30.4 nm @ 2^{nd}
60.9 nm @ 1^{st} order;</td></tr>
<tr><td colspan="2">EUV filter</td><td>Al filter</td><td>none</td></tr>
<tr><td colspan="2">UV filter</td><td>Interference Al/MgF$_2$</td><td>Interference Al/MgF$_2$ with clear aperture for the EUV spectrographic channel</td></tr>
<tr><td colspan="2">Filter wheel mechanism</td><td>yes</td><td>no</td></tr>
<tr><td colspan="2">UV detector openable door</td><td>yes</td><td>yes</td></tr>
</table>

Table 2 Main differences (in red) between the 4- and 3-channel instrument components

3.1 EUV Spectrographic Channel

The EUV spectrographic path of the 3-channel configuration maintains the same FOV (**Errore. L'origine riferimento non è stata trovata.**) and geometry of the 4-channel UV/EUV spectrographic path. The frequency of the SVLS grating is increased from 1800 l/mm to 3600 l/mm, and the HeII 30.4 nm radiation is diffracted at 2^{nd} order instead of at 4^{th} order.

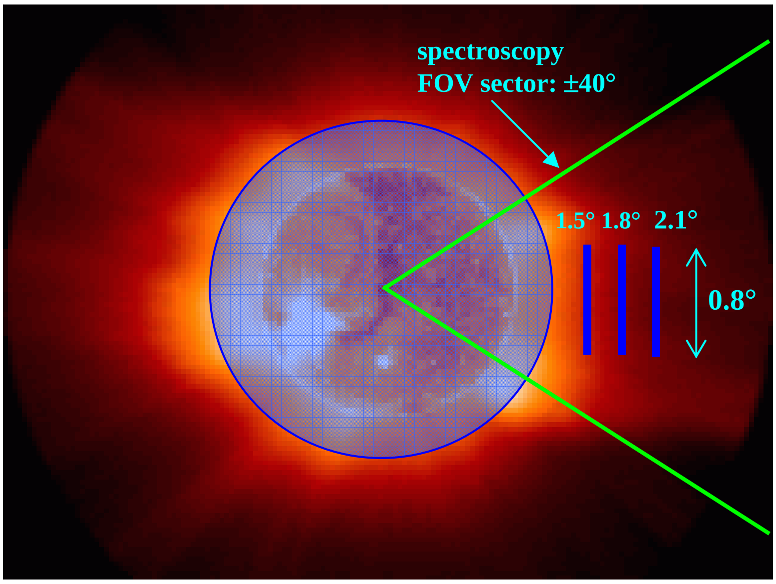

Figure 1 Multi-slits FOV at 0.28 AU for the EUV spectroscopic path. The FOV sector for spectroscopy is about ±40°. The remaining FOV is used for simultaneous imaging of visible-light pB and HI Ly-α. The spectrum is imaged on the portion of the detector that is not used to acquire the coronal image.

The HeII, 30.4 nm, at 2nd and the MgX, 60.9 nm, at 1st order are diffracted through an eccentric ~ ∅ 15 mm clear aperture on the ∅ 70 mm interference filter (Figure 2).

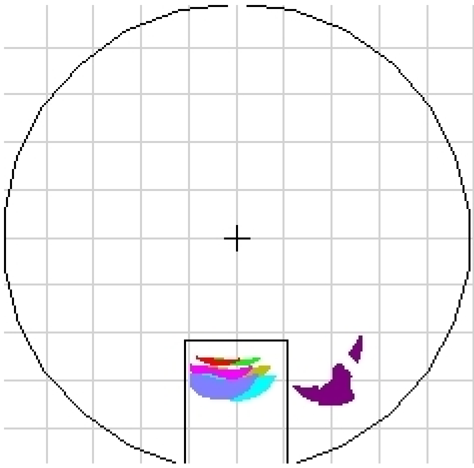

Figure 2 Interference filter with MgF_2 substrate and Al/MgF_2 coating for the VL- and UV imaging channels with clear aperture (bottom) for the EUV spectrographic channel

The grating diffracts at 1st order the HI Ly-α, 1216 nm, and the OVI doublet, 103.2/103.7 nm, outside of the focal plane into a light trap. (Figure 3)

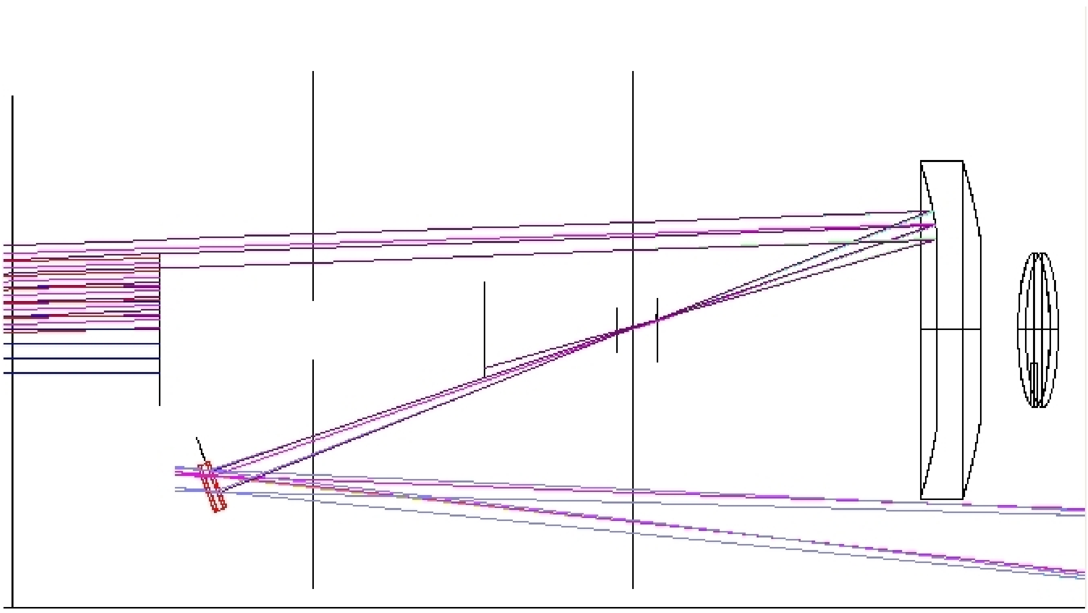

Figure 3 The grating diffracts at 1st order the HI Ly-α, 1216 nm, and the OVI doublet, 103.2/103.7 nm, outside of the focal plane into a light trap.

The optical specifications of the EUV spectrographic channel in the METIS 3-channel configuration are summarized in Table 3. In red are marked the differences from the 4-channel configuration (in parentheses).

Telescope Mirror	M1 sector illuminated by the coronal light going into the spectroscopy path		±40° (±32°)
Spectrometer	Entrance arm		250.0 mm
	Exit arm		500.0 mm
	Magnification		2.2
	Multislit	Slit # (FOVs)	3 (1.5°, 1.8°, 2.1°)
		Width	30 μm m (44 arcsec spatial resolution)
		Height (FOV)	1.5 mm (± 0.3°)
		Separation on the slit plane	0.72 mm
	Incidence angle (α)		≈0°
	Diffraction angle (β) 2nd order of 30.4 nm, 1st order of 60.9 nm		12.6°
SVLS grating	Ruled area		60 mm (// to the grooves) × 23 mm
	Radius		302.272 mm
	Central Ruling Frequency		3600 gr/mm (1800 gr/mm)
	Line Spacing Variation Factors (as defined in Zemax) T = lines/micron, y = distance fror grating center (mm) $1/T = 1/T_0 + \alpha y + \beta y^2 + \gamma y^3$	T_0	3.6
		α	1.27e-4
		β	-7.0e-7
		γ	0
Focal Plane	Pixel size		15 μm
	Spatial Plate Scale		10 arcsec/pixel
	Spectral Resolution (4-pixel resolution element = 30 μm slit-width × 2.2 magnification)		0.018 nm at 30.4 nm 0.037 nm at 60.9 nm
	Spectral separation between consecutive slits		0.44 nm at 30.4 nm 0.88 nm at 60.9 nm

Table 3 Optical specifications of the EUV spectroscopy path.

4 Instrument Sensitivity Estimate

The total instrument throughput derived from the component level efficiencies is shown in Table 4.

	4-channel		**3-channel**		
Optical Component	**Spectrography**	**Imaging**	**Spectrography**		**Imaging**
	4th ord. 30.4 nm	**121.6 nm**	**2nd ord. 30.4 nm**	**1st ord. 60.9 nm**	**121.6 nm**
Mo/Si ML reflectivity (M1)	0.2	0.34	0.2	0.12	0.34
Mo/Si ML reflectivity (M2)	N/A	0.34	N/A	N/A	N/A
Al/MgF_2 refletivity (M2)	N/A	N/A	N/A	N/A	0.88
Mo/Si ML reflectivity (grating)	0.2	N/A	0.2	0.12	N/A
Grating diffraction efficiency.	0.1	N/A	0.28	0.6	N/A
Filters transmission/reflectivity	0.3	0.2	N/A	N/A	0.2
Detector QE (KBr)	0.3	0.17	0.3	0.2	0.17
Total throughput	**3.6e-4**	**3.9e-3**	**3.4e-3**	**1.7e-3**	**1.0e-2**

Table 4 Efficiencies of the instrument optical components

4.1 Expected countrates

In order to verify that the overall performances of the METIS instrument meet the science requirements, the expected countrates (*i.e., counts-of-detected-photon/s/pixel*) have been estimated from typical coronal radiances (*photons/s/cm^2/sr*) in the three wavelength bandpasses of METIS. The instrument spatial plate scale is: 10 arcsec/pixel = 2.42 e-9 sr/pixel (cfr. Table 3)

- ### Countrates of imaging paths

The expected imaging countrates (*i.e., counts-of-detected-photon/s/pixel*) are given in Table 5(at 0.28 AU) and Table 6 (at 0.5AU).

		Streamer			**Coronal Hole**	
FOV [°]	$R_\odot$	121.6 nm (3-channel)	121,6 nm (4-channel)		121.6 nm (3-channel)	121,6 nm (4-channel)
1.50	1.58	3.95E+00	1.54E+00		4.31E-01	1.68E-01
1.80	1.89	4.69E+00	1.83E+00		3.33E-01	1.30E-01
2.10	2.21	3.79E+00	1.48E+00		2.15E-01	8.39E-02
2.40	2.52	2.82E+00	1.10E+00		1.36E-01	5.31E-02
2.70	2.84	1.97E+00	7.70E-01		7.62E-02	2.97E-02
3.00	3.16	1.33E+00	5.19E-01		4.28E-02	1.67E-02

Table 5 Estimated imaging countrates (count/s/pixel) at Solar minimum from perihelion at 0.28 AU

Streamer					Coronal Hole	
FOV [°]	$R_\odot$	121.6 nm (3-channel)	121.6 nm (4-channel)		121.6 nm (3-channel)	121.6 nm (4-channel)
1.50	2.82	1.56E-01	6.08E-02		6.08E-03	2.37E-03
1.80	3.38	2.01E-01	7.82E-02		5.79E-03	2.26E-03
2.10	3.94	1.58E-01	6.18E-02		2.59E-03	1.01E-03
2.40	4.51	1.10E-01	4.28E-02		7.23E-04	2.82E-04
2.70	5.07	7.28E-02	2.84E-02		1.53E-04	5.96E-05
3.00	5.64	4.51E-02	1.76E-02		2.90E-05	1.13E-05

Table 6 Estimated imaging countrates (count/s/pixel) at Solar minimum at 0.5 AU

- ## Countrates of the spectroscopy path

The expected imaging countrates (*i.e., counts-of-detected-photon/s/pixel*) are given in Table 7 (at 0.28 AU) and Table 8 (at 0.5AU).

Streamer					Coronal Hole	
Angle	Rsun	30.4 nm (3-channel)	30,4 nm (4-channel)		30.4 nm (3-channel)	30,4 nm (4-channel)
150	1.58	1.26E-01	1.33E-02		4.85E-03	5.13E-04
1.80	1.89	1.47E-01	1.56E-02		2.83E-03	3.00E-04
2.10	2.21	1.14E-01	1.21E-02		2.63E-03	2.78E-04

Table 7 Estimated spectroscopy countrates (count/s/pixel) at Solar minimum from perihelion at 0.28 AU

Streamer					Coronal Hole	
Angle	Rsun	30.4 nm (3-channel)	30,4 nm (4-channel)		30.4 nm (3-channel)	30,4 nm (4-channel)
1.50	2.82	4.40E-03	4.66E-04		1.48E-04	1.57E-05
1.80	3.38	4.63E-03	4.90E-04		2.93E-04	3.10E-05
2.10	3.94	2.93E-03	3.10E-04		3.43E-04	3.63E-05

Table 8 Estimated spectroscopy countrates (count/s/pixel) at Solar minimum at 0.5 AU

5 Conclusions

In the 3-channel configuration, the following instrument components are descoped:

1. Al filter;
2. filter wheel mechanism.

In this configuration, the spectrographic channel is maintained with the following modification, with respect to the 4-channel configuration:

1. SVLS grating 1800 l/mm ⇒ 3600 l/mm:
2. eccentric ∅ 15 mm clear aperture on the ∅ 70 mm interference filter.

In the 3-channel configuration, the UV and EUV throughputs increase by the following factors, with respect to the 4-channel:

1. factor of 2.5 increase for the UV-imaging,
2. factor of 9.4 increase for the EV spectrography.

6 Applicable Documents

6.1 Reference Documents

7 Acronyms

ADC	Analog to Digital Converter
AFT	Abbreviated Functional Test
AIT	Assembly, Integration and Test
AME	Absolute Maximum Error
AOCS	Attitude and Orbit Control System
AOI	
APE	Absolute Pointing Error
APS	Active Pixel Sensor
AU	Astronomical Unit
BB	Breadboard
BBM	Bread-Board Model
CCD	Charge Couple Device
CFRP	Carbon Fiber Reinforced Plastic
CME	Coronal Mass Ejections
CNR	Consiglio Nazionale delle Ricerche
CNRS	Centre National de la Recherche Scientifique
CoI	Co-Investigator
CoM	Center of Mass
CoPI	Co-Principal Investigator
COR	Baseline coronagraph proposed for METIS
CPI	Cross Products of Inertia
CTE	Coefficient of Thermal Expansion
DMS	Data Management System
DOF	Degree of freedom
ECSS	European Cooperation for Space Standardization
EDAC	Error Detection And Correction
EDWM	UV detector window mechanism
EEPROM	Electrically Erasable Programmable Random Access Memory
EEO	Extended External Occulter
EEOM	EEO Mechanism
EGSE	Electrical Ground Support Equipment
EM	Electrical Model
EM	Experiment Manager
EO	External occulter
EOM	External occulter Mechanism
EP	Entrance Pupil
EPROM	Erasable Programmable Random Access Memory
EQM	Electrical Qualification Model
ESA	European Space Agency

EUI	EUV Imager
EUV	Extreme UltraViolet
EUVC	EUV Channel
FDIR	Fault Detection, Isolation and Recovery
FEE	Front End Electronics
FEM	Filter Exchange Mechanism
FFT	Full Functional Test
FM	Flight Model
FOV	Field Of View
FPA	Focal Plane Assembly
FPGA	Field Programmable Gate Array
FS	Flight Spare
FWHM	Full Width at Half Maximum
GSE	Ground Support Equipment
H/W	Hardware
HeF	Aluminum low-pass filter of the coronagraph
HELEX	Heliophysical Explorers
HERSCHEL	Helium Resonance Scattering in the Corona and Heliosphere
HF	Narrow-band multilayer filter of the coronagraph
HGA	High Gain Antenna
HK	Housekeeping
HVPS	High Voltage Power Supply
HWRP	Half Wave Retarder Plate
IAC	Instituto de Astrofísica de Canarias
IAPS	Intensified Active pixel sensor
IAS	Institut d’Astrophysique Spatiale
IASF	Istituto di Astrofisica Spaziale e Fisica cosmica
IDP	Instrument Development Plan
IEO	Inverted External Occulter
IF	Interface
IFE	Instrument Front End
IFSI	Istituto di Fisica dello Spazio Interplanetario
ILS	Instrument Line of Sight
INAF	Istituto Nazionale di AstroFisica
INFM	Istituto Nazionale Fisica della Materia
IO	Internal Occulter
IOM	Internal Occulter Mechanism
IR	Infrared
LAM	Laboratoire d’Astrophysique de Marseille
LCL	Latching Current Limiters
LCVR	Liquid Crystal Variable Retarder
LOS	Line Of Sight
LS	Lyot Stop
LVPS	Low Voltage Power Supply
M0	Sun-disk rejection mirror of the coronagraph
M1	Primary mirror of the coronagraph
M2	Secondary mirror of the coronagraph
MCP	Micro Channel Plate
METIS	Multi Element Telescope for Imaging and Spectroscopy
MGSE	Mechanical Ground Support Equipment
ML	Multilayer

MOC	Mission Operation Center
MoI	Moment of Inertia
MOM	Pag. 58
MPPU	METIS Processing & Power Unit
MPS	Max-Planck-Institut fuer Sonnensystemforschung
MSSL	Mullard Space Science Laboratory
N/A	Not Applicable
NASA	National Areonautics and Space Administration
NOM	Nominal Observing Mode
NRL	Naval Research Laboratory
OAA	Osservatorio Astronomico di Arcetri
OACN	Osservatorio Astronomico di Capodimonte Napoli
OACt	Osservatorio Astronomico di Catania
OAPa	Osservatorio Astronomico di Palermo
OAR	Osservatorio Astronomico di Roma
OATo	Osservatorio Astronomico di Torino
OATs	Osservatorio Astronomico di Trieste
OGSE	Optical Ground Support Equipment
OP	Off Pointing
PA	Product Assurance
PI	Principal Investigator
PMP	Polarization Modulation Package
PoliTo	Politecnico di Torino
POS	Polarization Optics System
PROM	Programmable Read Only Memory
QE	Quantum Efficiency
RD-n	Reference Document n
ROIC	Read Out Integrated Circuit
ROS	Relay Optics System
RPE	Relative Pointing Error
S/C	Spacecraft
S/W	Software
SCORE	Sounding-rocket Coronagraphic Experiment
SEA	Shield Entrance Aperture
SEP	Solar Energetic Particles
SMM	Structural Mathematical Model
SO	Solar Orbiter
SOHO	Solar and Heliospheric Observatory
SpW	Space Wire
STOM	Structural Thermal Optical Model
SVLS	Spherical Varied Line-spaced
TBC	To Be Confirmed
TBD	To Be Defined
TBW	To Be Written
TC	Tele Command
TEC	Thermo Electric Coooler
TLM	Telemetry
TM	Telemetry
TSOM	Time Share Observing Mode
TVLS	Toroidal Varied Line-spaced
UFOV	Unobstructed Field Of View

UniAq	Università di Aquila
UniCal	Università della Calabria
UniFi	Università di Firenze
UniPD	Università di Padova
UniPd	Università di Padova
UniPg	Università di Perugia
UniPv	Università di Pavia
UniRm	Università di Roma
UORF	Unit Optical Reference Frame
URF	Unit Reference Frame
UV	Ultraviolet
UVC	UV channel
UVD	Ultraviolet Detector
VD	Visible Detector
VIM	Visible Imager & Magnetograph
VL	Visible-light
VLC	Visible Light Channel
VUV	Vacuum ultraviolet

METIS 3-channel Configuration

DRAFT

Silvano Fineschi
INAF – Astrophysical Observatory of Turin, Torino, Italy

issue	0
revision	0– draft 1
date of issue	15 July 2012

Page intentionally left blank

Distribution

Name	Organisation

Change Log

date	issue	revision	Paragraphs	reason for change
15/07/12	0	0	All	First release

Table of Contents

LIST OF FIGURES

LIST OF TABLES

1 Abstract

This document describes the 3-channel configuration of the METIS experiment. This configuration has been derived from the original 4-channel configuration as a consequence of the descoping of the He-imaging channel decided by ASI during the coordination meeting with Thales-Alenia Space on July the 13th, 2012.
In the 3-channel configuration, the following instrument components are descoped:

1. Al filter;
2. filter wheel mechanism.

In this configuration, the spectrographic channel is maintained with the following modification, with respect to the 4-channel configuration:

1. SVLS grating 1800 l/mm ⇒ 3600 l/mm:
2. eccentric ∅ 15 mm clear aperture on the ∅ 70 mm interference filter.

In the 3-channel configuration, the UV and EUV throughputs increase by the following factors, with respect to the 4-channel:

1. factor of 2.5 increase for the UV-imaging,
2. factor of 9.4 increase for the EV spectrography.

2 Revised 3-channel Experiment Science Objectives

The baseline 4-channel Multi-Element Telescope for Imaging and Spectroscopy - METIS – for the Solar Orbiter mission was designed to combine the imaging and spectroscopic capabilities of coronagraphs and spectrometers. With respect to the original METIS 4-channel configuration, the 3-channel configuration loses the HeII Ly-α imaging and the HI Ly-α spectrography, while it maintains the visible-light pB imaging, the HI Ly-α imaging and the HeII Ly-α spectrography. In addition, unlike in the 4-channel METIS, the 3-channel configuration may include also the MgX, 60.9 nm, spectrography.

Table 1 summarizes the different science performances of the 4- and 3-channel configurations.

4-channel	3-channel
linearly polarized K-corona imaging (590-650 nm)	linearly polarized K-corona imaging (590-650 nm)
narrow-band UV imaging HI Lyman α (121.6 nm)	narrow-band UV imaging HI Lyman α (121.6 nm)
narrow-band extreme UV imaging HeII (30.4 nm)	descoped
spectrography HI 121.6 nm (1st) HeII 30.4 nm (4th)	spectrography HeII 30.4 nm (2nd) MgX 60.9 nm (1st)

Table 1 Science performances of the 4- and 3-channel METIS configurations

3 Instrument Parameters

Table 2 summarizes the main differences (in red) between the 4- and 3-channel instrument components.

Instrument Component		**4-channel METIS configuration**	**3-channel METIS configuration**
M1 coating		UV-capped multilayer @ 30 nm	UV-capped multilayer @ 30 nm
M2 coating		UV-capped multilayer @ 30 nm	Interference coating Al/MgF_2 @ 122 nm
SVLS grating	coating	UV-capped multilayer @ 30 nm	multilayer @ 30 nm (no UV-cap required)
	ruling frequency	1800 lines/mm	3600 lines/mm
	wavelengths	30.4 nm @ 4^{th} 121.6 nm @ 1^{st} order;	30.4 nm @ 2^{nd} 60.9 nm @ 1^{st} order;
EUV filter		Al filter	none
UV filter		Interference Al/MgF_2	Interference Al/MgF_2 with clear aperture for the EUV spectrographic channel
Filter wheel mechanism		yes	no
UV detector openable door		yes	yes

Table 2 Main differences (in red) between the 4- and 3-channel instrument components

3.1 EUV Spectrographic Channel

The EUV spectrographic path of the 3-channel configuration maintains the same FOV (**Errore. L'origine riferimento non è stata trovata.**) and geometry of the 4-channel UV/EUV spectrographic path. The frequency of the SVLS grating is increased from 1800 l/mm to 3600 l/mm, and the HeII 30.4 nm radiation is diffracted at 2^{nd} order instead of at 4^{th} order.

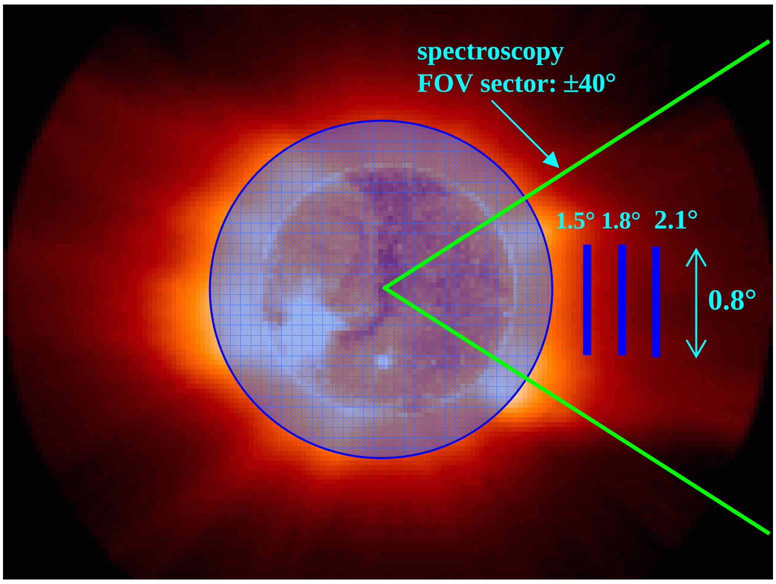

Figure 1 Multi-slits FOV at 0.28 AU for the EUV spectroscopic path. The FOV sector for spectroscopy is about ±40°. The remaining FOV is used for simultaneous imaging of visible-light pB and HI Ly-α. The spectrum is imaged on the portion of the detector that is not used to acquire the coronal image.

The HeII, 30.4 nm, at 2nd and the MgX, 60.9 nm, at 1st order are diffracted through an eccentric ~ ∅ 15 mm clear aperture on the ∅ 70 mm interference filter (Figure 2).

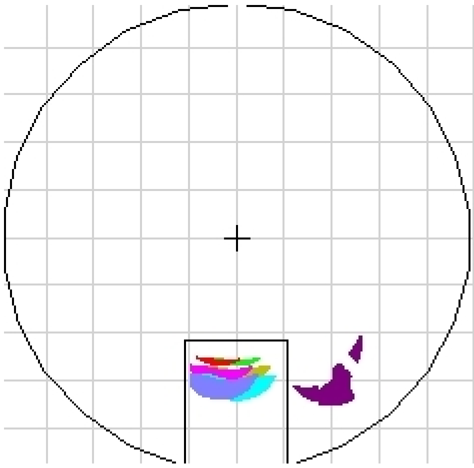

Figure 2 Interference filter with MgF_2 substrate and Al/MgF_2 coating for the VL- and UV imaging channels with clear aperture (bottom) for the EUV spectrographic channel

The grating diffracts at 1st order the HI Ly-α, 1216 nm, and the OVI doublet, 103.2/103.7 nm, outside of the focal plane into a light trap. (Figure 3)

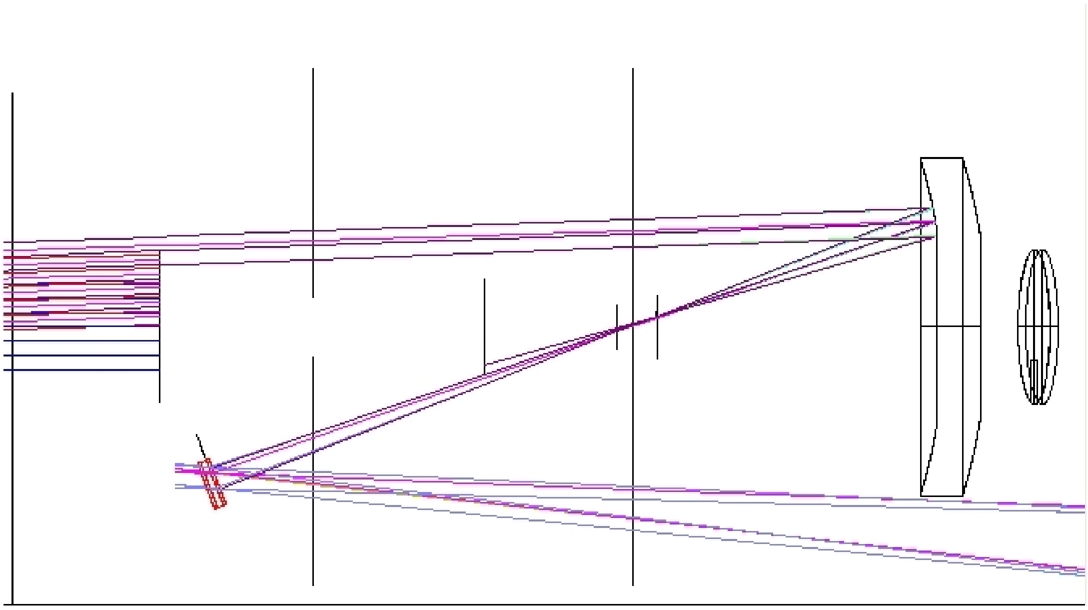

Figure 3 The grating diffracts at 1st order the HI Ly-α, 1216 nm, and the OVI doublet, 103.2/103.7 nm, outside of the focal plane into a light trap.

The optical specifications of the EUV spectrographic channel in the METIS 3-channel configuration are summarized in Table 3. In red are marked the differences from the 4-channel configuration (in parentheses).

Telescope Mirror	M1 sector illuminated by the coronal light going into the spectroscopy path		±40° (±32°)
Spectrometer	Entrance arm		250.0 mm
	Exit arm		500.0 mm
	Magnification		2.2
	Multislit	Slit # (FOVs)	3 (1.5°, 1.8°, 2.1°)
		Width	30 μm m (44 arcsec spatial resolution)
		Height (FOV)	1.5 mm (± 0.3°)
		Separation on the slit plane	0.72 mm
	Incidence angle (α)		≈0°
	Diffraction angle (β) 2nd order of 30.4 nm, 1st order of 60.9 nm		12.6°
SVLS grating	Ruled area		60 mm (// to the grooves) × 23 mm
	Radius		302.272 mm
	Central Ruling Frequency		3600 gr/mm (1800 gr/mm)
	Line Spacing Variation Factors (as defined in Zemax) T = lines/micron, y = distance from grating center (mm) $1/T = 1/T_0 + \alpha y + \beta y^2 + \gamma y^3$	T_0	3.6
		α	1.27e-4
		β	-7.0e-7
		γ	0
Focal Plane	Pixel size		15 μm
	Spatial Plate Scale		10 arcsec/pixel
	Spectral Resolution (4-pixel resolution element = 30 μm slit-width × 2.2 magnification)		0.018 nm at 30.4 nm 0.037 nm at 60.9 nm
	Spectral separation between consecutive slits		0.44 nm at 30.4 nm 0.88 nm at 60.9 nm

Table 3 Optical specifications of the EUV spectroscopy path.

4 Instrument Sensitivity Estimate

The total instrument throughput derived from the component level efficiencies is shown in Table 4.

	4-channel		3-channel		
Optical Component	Spectrography	Imaging	Spectrography		Imaging
	4^{th} ord. 30.4 nm	121.6 nm	2^{nd} ord. 30.4 nm	1^{st} ord. 60.9 nm	121.6 nm
Mo/Si ML reflectivity (M1)	0.2	0.34	0.2	0.12	0.34
Mo/Si ML reflectivity (M2)	N/A	0.34	N/A	N/A	N/A
Al/MgF_2 refletivity (M2)	N/A	N/A	N/A	N/A	0.88
Mo/Si ML reflectivity (grating)	0.2	N/A	0.2	0.12	N/A
Grating diffraction efficiency.	0.1	N/A	0.28	0.6	N/A
Filters transmission/reflectivity	0.3	0.2	N/A	N/A	0.2
Detector QE (KBr)	0.3	0.17	0.3	0.2	0.17
Total throughput	**3.6e-4**	**3.9e-3**	**3.4e-3**	**1.7e-3**	**1.0e-2**

Table 4 Efficiencies of the instrument optical components

4.1 Expected countrates

In order to verify that the overall performances of the METIS instrument meet the science requirements, the expected countrates (*i.e., counts-of-detected-photon/s/pixel*) have been estimated from typical coronal radiances (*photons/s/cm^2/sr*) in the three wavelength bandpasses of METIS. The instrument spatial plate scale is: 10 arcsec/pixel = 2.42 e-9 sr/pixel (cfr. Table 3)

- **Countrates of imaging paths**

The expected imaging countrates (*i.e., counts-of-detected-photon/s/pixel*) are given in Table 5(at 0.28 AU) and Table 6 (at 0.5AU).

		Streamer			Coronal Hole	
FOV [°]	$R_\odot$	121.6 nm (3-channel)	121,6 nm (4-channel)		121.6 nm (3-channel)	121,6 nm (4-channel)
1.50	1.58	3.95E+00	1.54E+00		4.31E-01	1.68E-01
1.80	1.89	4.69E+00	1.83E+00		3.33E-01	1.30E-01
2.10	2.21	3.79E+00	1.48E+00		2.15E-01	8.39E-02
2.40	2.52	2.82E+00	1.10E+00		1.36E-01	5.31E-02
2.70	2.84	1.97E+00	7.70E-01		7.62E-02	2.97E-02
3.00	3.16	1.33E+00	5.19E-01		4.28E-02	1.67E-02

Table 5 Estimated imaging countrates (count/s/pixel) at Solar minimum from perihelion at 0.28 AU

		Streamer			Coronal Hole	
FOV [°]	$R_\odot$	121.6 nm (3-channel)	121.6 nm (4-channel)		121.6 nm (3-channel)	121.6 nm (4-channel)
1.50	2.82	1.56E-01	6.08E-02		6.08E-03	2.37E-03
1.80	3.38	2.01E-01	7.82E-02		5.79E-03	2.26E-03
2.10	3.94	1.58E-01	6.18E-02		2.59E-03	1.01E-03
2.40	4.51	1.10E-01	4.28E-02		7.23E-04	2.82E-04
2.70	5.07	7.28E-02	2.84E-02		1.53E-04	5.96E-05
3.00	5.64	4.51E-02	1.76E-02		2.90E-05	1.13E-05

Table 6 Estimated imaging countrates (count/s/pixel) at Solar minimum at 0.5 AU

- ## Countrates of the spectroscopy path

The expected imaging countrates (*i.e.*, *counts-of-detected-photon/s/pixel*) are given in Table 7 (at 0.28 AU) and Table 8 (at 0.5AU).

		Streamer			Coronal Hole	
Angle	Rsun	30.4 nm (3-channel)	30,4 nm (4-channel)		30.4 nm (3-channel)	30,4 nm (4-channel)
150	1.58	1.26E-01	1.33E-02		4.85E-03	5.13E-04
1.80	1.89	1.47E-01	1.56E-02		2.83E-03	3.00E-04
2.10	2.21	1.14E-01	1.21E-02		2.63E-03	2.78E-04

Table 7 Estimated spectroscopy countrates (count/s/pixel) at Solar minimum from perihelion at 0.28 AU

		Streamer			Coronal Hole	
Angle	Rsun	30.4 nm (3-channel)	30,4 nm (4-channel)		30.4 nm (3-channel)	30,4 nm (4-channel)
1.50	2.82	4.40E-03	4.66E-04		1.48E-04	1.57E-05
1.80	3.38	4.63E-03	4.90E-04		2.93E-04	3.10E-05
2.10	3.94	2.93E-03	3.10E-04		3.43E-04	3.63E-05

Table 8 Estimated spectroscopy countrates (count/s/pixel) at Solar minimum at 0.5 AU

5 Conclusions

In the 3-channel configuration, the following instrument components are descoped:

1. Al filter;
2. filter wheel mechanism.

In this configuration, the spectrographic channel is maintained with the following modification, with respect to the 4-channel configuration:

1. SVLS grating 1800 l/mm ⇒ 3600 l/mm:
2. eccentric ∅ 15 mm clear aperture on the ∅ 70 mm interference filter.

In the 3-channel configuration, the UV and EUV throughputs increase by the following factors, with respect to the 4-channel:

1. factor of 2.5 increase for the UV-imaging,
2. factor of 9.4 increase for the EV spectrography.

6 Applicable Documents

6.1 Reference Documents

7 Acronyms

ADC	Analog to Digital Converter
AFT	Abbreviated Functional Test
AIT	Assembly, Integration and Test
AME	Absolute Maximum Error
AOCS	Attitude and Orbit Control System
AOI	
APE	Absolute Pointing Error
APS	Active Pixel Sensor
AU	Astronomical Unit
BB	Breadboard
BBM	Bread-Board Model
CCD	Charge Couple Device
CFRP	Carbon Fiber Reinforced Plastic
CME	Coronal Mass Ejections
CNR	Consiglio Nazionale delle Ricerche
CNRS	Centre National de la Recherche Scientifique
CoI	Co-Investigator
CoM	Center of Mass
CoPI	Co-Principal Investigator
COR	Baseline coronagraph proposed for METIS
CPI	Cross Products of Inertia
CTE	Coefficient of Thermal Expansion
DMS	Data Management System
DOF	Degree of freedom
ECSS	European Cooperation for Space Standardization
EDAC	Error Detection And Correction
EDWM	UV detector window mechanism
EEPROM	Electrically Erasable Programmable Random Access Memory
EEO	Extended External Occulter
EEOM	EEO Mechanism
EGSE	Electrical Ground Support Equipment
EM	Electrical Model
EM	Experiment Manager
EO	External occulter
EOM	External occulter Mechanism
EP	Entrance Pupil
EPROM	Erasable Programmable Random Access Memory
EQM	Electrical Qualification Model
ESA	European Space Agency

EUI	EUV Imager
EUV	Extreme UltraViolet
EUVC	EUV Channel
FDIR	Fault Detection, Isolation and Recovery
FEE	Front End Electronics
FEM	Filter Exchange Mechanism
FFT	Full Functional Test
FM	Flight Model
FOV	Field Of View
FPA	Focal Plane Assembly
FPGA	Field Programmable Gate Array
FS	Flight Spare
FWHM	Full Width at Half Maximum
GSE	Ground Support Equipment
H/W	Hardware
HeF	Aluminum low-pass filter of the coronagraph
HELEX	Heliophysical Explorers
HERSCHEL	Helium Resonance Scattering in the Corona and Heliosphere
HF	Narrow-band multilayer filter of the coronagraph
HGA	High Gain Antenna
HK	Housekeeping
HVPS	High Voltage Power Supply
HWRP	Half Wave Retarder Plate
IAC	Instituto de Astrofísica de Canarias
IAPS	Intensified Active pixel sensor
IAS	Institut d'Astrophysique Spatiale
IASF	Istituto di Astrofisica Spaziale e Fisica cosmica
IDP	Instrument Development Plan
IEO	Inverted External Occulter
IF	Interface
IFE	Instrument Front End
IFSI	Istituto di Fisica dello Spazio Interplanetario
ILS	Instrument Line of Sight
INAF	Istituto Nazionale di AstroFisica
INFM	Istituto Nazionale Fisica della Materia
IO	Internal Occulter
IOM	Internal Occulter Mechanism
IR	Infrared
LAM	Laboratoire d'Astrophysique de Marseille
LCL	Latching Current Limiters
LCVR	Liquid Crystal Variable Retarder
LOS	Line Of Sight
LS	Lyot Stop
LVPS	Low Voltage Power Supply
M0	Sun-disk rejection mirror of the coronagraph
M1	Primary mirror of the coronagraph
M2	Secondary mirror of the coronagraph
MCP	Micro Channel Plate
METIS	Multi Element Telescope for Imaging and Spectroscopy
MGSE	Mechanical Ground Support Equipment
ML	Multilayer

MOC	Mission Operation Center
MoI	Moment of Inertia
MOM	Pag. 58
MPPU	METIS Processing & Power Unit
MPS	Max-Planck-Institut fuer Sonnensystemforschung
MSSL	Mullard Space Science Laboratory
N/A	Not Applicable
NASA	National Areonautics and Space Administration
NOM	Nominal Observing Mode
NRL	Naval Research Laboratory
OAA	Osservatorio Astronomico di Arcetri
OACN	Osservatorio Astronomico di Capodimonte Napoli
OACt	Osservatorio Astronomico di Catania
OAPa	Osservatorio Astronomico di Palermo
OAR	Osservatorio Astronomico di Roma
OATo	Osservatorio Astronomico di Torino
OATs	Osservatorio Astronomico di Trieste
OGSE	Optical Ground Support Equipment
OP	Off Pointing
PA	Product Assurance
PI	Principal Investigator
PMP	Polarization Modulation Package
PoliTo	Politecnico di Torino
POS	Polarization Optics System
PROM	Programmable Read Only Memory
QE	Quantum Efficiency
RD-n	Reference Document n
ROIC	Read Out Integrated Circuit
ROS	Relay Optics System
RPE	Relative Pointing Error
S/C	Spacecraft
S/W	Software
SCORE	Sounding-rocket Coronagraphic Experiment
SEA	Shield Entrance Aperture
SEP	Solar Energetic Particles
SMM	Structural Mathematical Model
SO	Solar Orbiter
SOHO	Solar and Heliospheric Observatory
SpW	Space Wire
STOM	Structural Thermal Optical Model
SVLS	Spherical Varied Line-spaced
TBC	To Be Confirmed
TBD	To Be Defined
TBW	To Be Written
TC	Tele Command
TEC	Thermo Electric Coooler
TLM	Telemetry
TM	Telemetry
TSOM	Time Share Observing Mode
TVLS	Toroidal Varied Line-spaced
UFOV	Unobstructed Field Of View

UniAq	Università di Aquila
UniCal	Università della Calabria
UniFi	Università di Firenze
UniPD	Università di Padova
UniPd	Università di Padova
UniPg	Università di Perugia
UniPv	Università di Pavia
UniRm	Università di Roma
UORF	Unit Optical Reference Frame
URF	Unit Reference Frame
UV	Ultraviolet
UVC	UV channel
UVD	Ultraviolet Detector
VD	Visible Detector
VIM	Visible Imager & Magnetograph
VL	Visible-light
VLC	Visible Light Channel
VUV	Vacuum ultraviolet